Development of Materials for Thermoelectric Generators: Superlattice $Ca_3Co_4O_9$-$Sr_3Co_4O_9$

Shapoval O., Belenchuk A.
IEEN, ASM
Chisinau, Moldova
oleg.shapoval@nano.asm.com

Jooss C., Roddatis V.
IMP, Uni-Goettingen
Goettingen, Germany

V. Moshnyaga
I Phys.Institut, Uni-Goettingen
Goettingen, Germany

***Abstract* – We have prepared multilayered structures composed from misfit layered Ca- and Sr- cobaltates by Metalorganic Aerosol Deposition technique. X-ray and Transmission Electron Microscopy analyzes confirms the forming superlattice along c direction from common CoO_2 interlayers and alternating Ca_2CoO_3 and Sr_2CoO_3 layers with periodicity of 4-6 unit cell. Our results indicate the possibility to fabricate artificial material on the base of layered cobaltates for thermoelectric applications.**

***Index Terms* – Metalorganic aerosol deposition, thermoelectric oxide material, superlattice, transmission electron microscopy.**

I. Introduction

The development of oxide materials science has led to oxides invasion in the thermoelectrics until recently an area of semiconductors application exclusively [1]. The well-established semiconducting alloys, such as Bi_2Te_3, PbTe, Bi–Sb, and Si–Ge, which are being used in thermoelectric (TE) devices, have many limitations that are low decomposition temperature and presence of toxic elements. Increasing interest have been focused at last years on oxide materials because their natural abundance, non-toxicity and remarkable thermal and chemical stabilities at high temperatures [2].

The misfit layered $Ca_3Co_4O_9$ (CCO) is among the most promising p-type oxide materials for high temperature TE applications, with the figure-of-merit (ZT) obtained for a single crystals reaching as high as 0.87 at 1000 K [3]. Phonon scattering due to large in-plane atomic displacement in the Ca_2CoO_3 layers ("phonon glass") and preservation of high electric conductivity within the crystalline CoO_2 layers ("electron crystal") is the reason why CCO efficiently converts heat to electricity [5]. The crystal structure of CCO is shown on Fig.1.

The enhancement of functionality of oxides based material can be achieved by building artificial atomic-scale tailored structure, for example superlattice (SL) [6]. Naturally layered cobaltates seem a good candidate for material engineering. The metastable layered cobaltate $Sr_3Co_4O_9$ (SCO) [7] have the same crystal structure as CCO with slightly different lattice parameters (see TABLE I.).

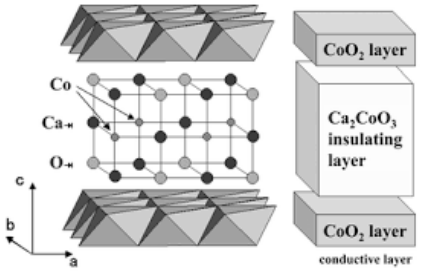

Fig. 1. Crystal structure of layered Ca3Co4O9 [4]

The most significant differences are observed between Ca_2CoO_3 and Sr_2CoO_3 layers. Mismatch $\Delta a/a$ and $\Delta b_1/b_1$ are 1.7% and 7.7%, respectively. Whereas mismatch between lattice parameter of CoO_2 interlayers in both compounds $\Delta b_2/b_2$ is 0.35%. The superlattice can be built along ***c*** direction from common CoO_2 interlayers and alternating with some periodicity Ca_2CoO_3 and Sr_2CoO_3 layers. Thus strong mismatched layer will be uncoupled due to identical CoO_2 layers. One can expect the reduction of thermal conductivity in the SL due to additional degree of freedom at conservation of high conductivity in CoO_2 layers.

II. Experiment

The samples of films and multilayered structures were prepared by Metalorganic Aerosol Deposition (MAD) technique [8] . The CCO and SCO films were deposited from aerosols of organic solutions, containing mixture of both metal β- diketonates (e.g. Ca- and Co-acetylacetonates). We used standard technique [9] for the preparation of atomically smooth TiO_2-terminated $SrTiO_3$(100) (STO) substrate with terrace steps of one unit cell in height. The ratio Ca/Co in solution has been varied to adjust the formation layered CCO without presence of CaO and Co_3O_4 precipitates. We have

TABLE I. CELL PARAMETERS OF LAYERED COBALTATES

	a, nm	*b_1, nm*	*b_2, nm*	*c, nm*	*Ref.*
CCO	0.483	0.456	0.282	1.084	[10]
SCO	0.491	0.496	0.283	1.090	[7]

explored MAD growth conditions for deposition of CCO (SCO) films with out-of-plane c axis orientation only.

The CCO-SCO multilayered structures was grown on substrate heated to T_{sub}=800°C. Epitaxial multilayered structure was formed in result of sequential spraying of aerosols of two organic solutions containing metalorganic precursors. CCO layers grew from mixture of Ca-and Co-acetylacetonates and SCO layers were derived from Sr- and Co-acetylacetonate. Deposition chamber was equipped by ellipsometry measurement system for monitoring of the growth process. The monolayer accuracy was achieved by accurate calibration of dosing units.

Two CCO-SCO multilayered structures with different periods have been fabricated. The individual thickness ratio between CCO and SCO layers was about 1:1. Number of repetition was 12 and 20 in order to provide overall thickness of structures about 85 nm.

The film surface morphology was examined by a scanning tunneling microscope (STM) in a Veeco Multimode V Scanning Probe Microscope. The SL structures were determined by a small-angle X-ray reflectivity (XRD) and X-ray diffraction (XRD) in a Siemens D5000 diffractometer. Electron transport measurements were performed by standard 4-probe technique using commercial PPMS from "Quantum Design". The atomic-resolution TEM images were obtained using a Titan E-TEM (environmental transmission electron microscope).

III. STRUCTURE OF CCO-SCO SUPERLATTICES

A. X-ray diffraction

The synthesized structures were examined by X-ray analysis. Fig.2(a) shows θ-2θ X-ray diffraction overview spectra. The overall thicknesses of 12 and 20 periods SLs calculated from Kiessig fringes are 86.0 nm and 82.5 nm (see X-ray reflection spectra on Fig.2(b)). One can see first order (1_1 and1_2) of Bragg reflection due to the superlattice structure. The evidence for a SL formation is confirmed by well-formed satellite peaks in XRD patterns for all prepared structures. The same individual thickness ratio and, presumably, absence of strain in SLs led to equal positions of SL0(X00) Bragg peaks in both structure. The average lattice parameter of SLs ***c***=1.086 nm ranges between ***c*** parameters of CCO and SCO.

The SL periods were calculated from satellite peak positions $(2\sin\theta_{SLn}-2\sin\theta_{SL0})=\pm n\lambda/T$, where λ is the X-ray wavelength, n is the order of satellite peaks, θ_{SLn} is the diffraction angle of the satellite peak, and θ_{SL0} is the Bragg angle of the host lattice (Fig.2.(c)). Calculated periods are equal to 7.05 nm and 3.83 nm. The Laue fringes around (100) Bragg peak of SLs (Fig.2.(d)) also infer a good crystal quality of grown structures. The thicknesses associated with their periodicity are 84.0 nm and 79.0 nm.

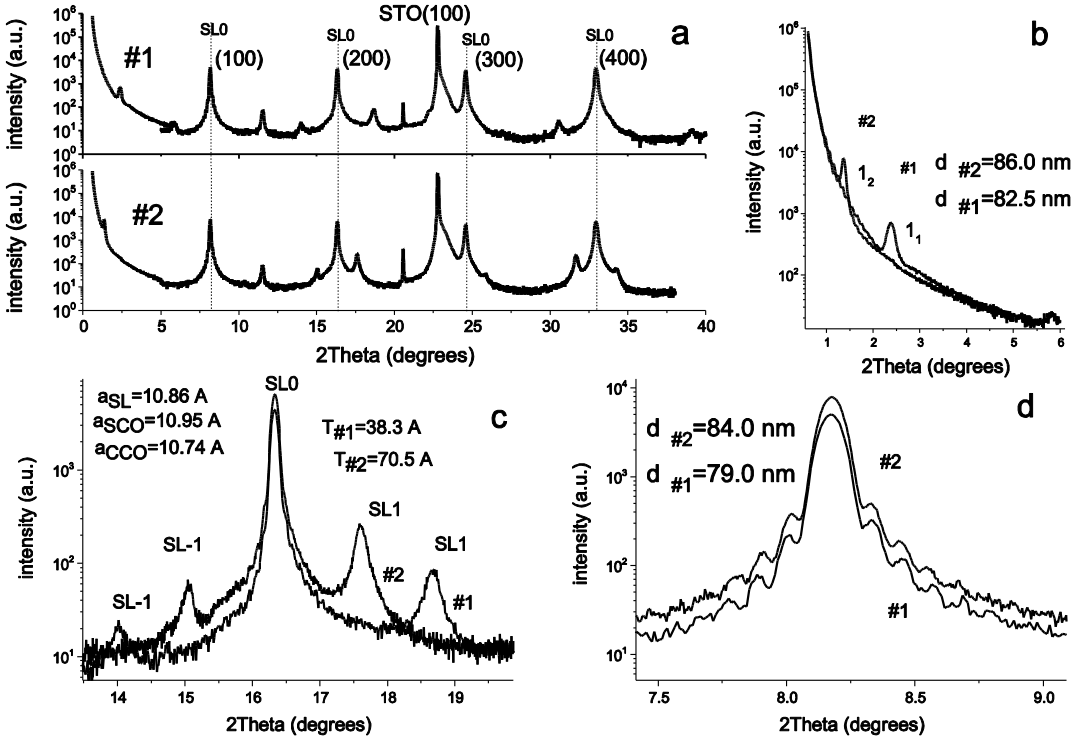

Fig. 2. X-ray analysis of CCO-SCO SLs: #1 – 20 periods SL, #2 – 12 periods SL. (a) overview XRD spectra; (b) XRR spectra; (c) XRD spectra around (200) Bragg peak of SL; (d) Laue fringes around (100) Bragg peak of SL.

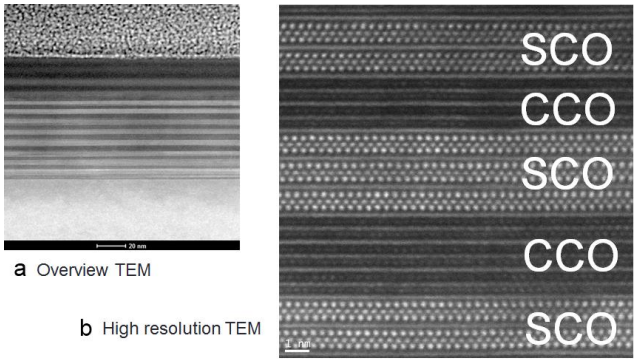

Fig. 3. Low magnification (a) and high resolution (b) TEM images of 12 periods CCO-SCO superlattice.

Thicknesses of SLs calculated from XRR data is differ from defined from XRD one. This difference in calculations can be explained from origin of fringes on XRR and XRD patterns. In XRD case oscillations emerge from the crystalline structure, while in XRR fringes originate from the presence of two interfaces, independent of the crystallinity of the material in between. Consequently, the XRD fringes are extremely sensitive on the qualities of the interface while the Laue oscillations depend only weakly on properties like surface roughness but are sensitive to crystalline disorder. Therefore, the two provide complementary information: the XRR fringes determine the total thickness of a sample, while the XRD oscillations probe the size of the crystalline ordered volume.

B. TEM

Figure 3(a) shows cross-sectional TEM overview image of CCO-SCO SL grown on STO(100) substrate. The flat structure about 84 nm thick is formed by 12 pairs of CCO and SCO layered parallel to substrate. Detailed structure of SL are clearly visible on the high resolution TEM image (Fig.3(b)). The CoO_2 layers (light grey stripes) alternate through whole cross section with period of one unite cell about 1.1 nm. Between CoO_2 layers settle three units of rocksalt blocks Ca_2CoO_3 or Sr_2CoO_3 which form CCO or SCO individual layers of SL.

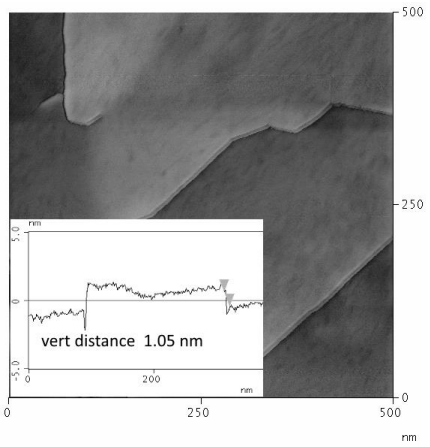

Fig. 4. STM image of surface of CCO-SCO superlattice. Insert shows profile along diagonal of scan.

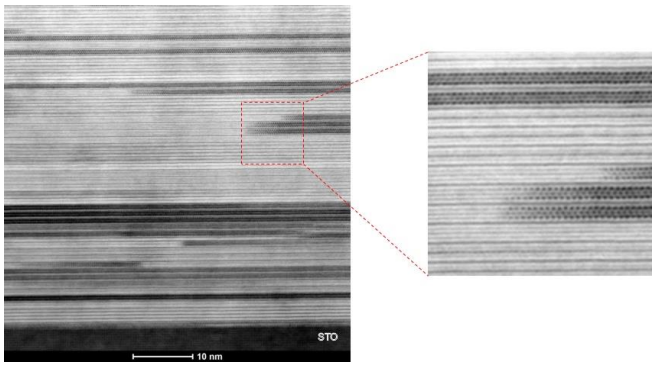

Fig. 5. Bright field TEM images of CCO-SCO superlattice. The insert marks out the rotation of rocksalt interlayers.

The periods calculated from XRD measurements are 7.05 nm and 3.83 nm for 12 and 20 periods SL and don't multiple to one unit cell parameter and are result of integral average values. As seen from TEM image the 12 periods multilayer structure is consisted locally from 2/4, 3/3, 3/4 or 4/3 of CCO/SCO monolayers. Bright field high resolution TEM mode (Fig.4) clearly exhibits at least the two type of defect of structure in SL, which don't lead to forming grains due to incommensurate structure of layered cobaltates. The rocksalt interlayers undergo rotation in-plane despite on rigorous arrangement of CoO_2 layers (see insert on Fig.4). Also one can observe material contrast within a rocksalt layer when succeeding Sr_2CoO_3 start growth on steps of previous Ca_2CoO_3 and other way round.

C. STM

STM surface analysis is presented on Fig. 6. The surface of CCO-SCO SL clearly demonstrates flat terraces of about 200 nm width and a one unite cell ***c*** height (~1.05 nm).

IV. Electric properties

The electrical resistance of the samples was measured by the four-probe method along the directions parallel to the CoO_2 layers. The resistivity of a flat sample can be easily estimated as $\rho=Rd$, where d is the thickness of the thin film.

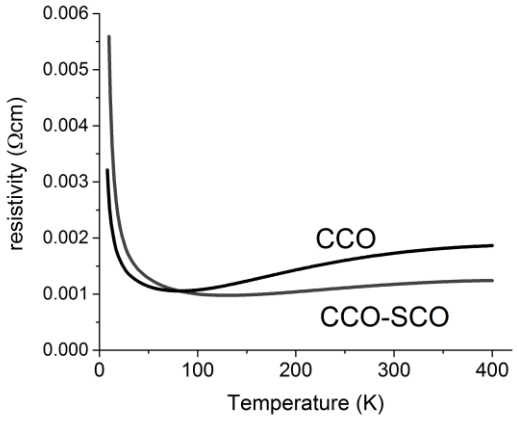

Fig. 6. Temperature dependence of resistivity of CCO single film and CCO-SCO structure.

Figure 6 shows the temperature dependence of the resistivity for CCO film and CCO-SCO SL grown on STO(100) substrates. The resistivity of SL exhibits a metallic behavior similar to CCO, but in contrast to CCO the SL shows metal-insulator transition at higher temperature 120 K and its room-temperature resistivity is lower.

We can expect that due to lower electric resistivity parallel to the CoO_2 layers in SL the thermoelectric power factor should be considerable larger than that of CCO.

V. Conclusion

MAD allows fabrication of artificial oxide materials with specific properties by atomic-scale tailoring of their composition. The epitaxial growth of layered cobaltates based SLs is possible on mismatched STO(100) substrates. The CCO-SCO SLs on STO(100) substrate exhibits overall high crystal quality and are in accordance with suggested model.

The proposed SL has potential advantage in search for thermoelectric materials of higher performance. Future measurements of thermal conductivity of SL will have to clarify its applicability as component for thermoelectric devices.

Acknowledgment

Financial support from the SFB 1073 is acknowledged.

References

[1] C. Han, Z. Li, and S. Dou, "Recent progress in thermoelectric materials," *Chin. Sci. Bull.*, vol. 59, no. 18, pp. 2073–2091, Jun. 2014.

[2] J. He, Y. Liu, and R. Funahashi, "Oxide thermoelectrics: The challenges, progress, and outlook," *J. Mater. Res.*, vol. 26, no. 15, pp. 1762–1772, 2011.

[3] M. Shikano and R. Funahashi, "Electrical and thermal properties of single-crystalline $(Ca_2CoO_3)_{0.7}CoO_2$ with a $Ca_3Co_4O_9$ structure," *Appl. Phys. Lett.*, vol. 82, no. 12, pp. 1851–1853, Mar. 2003.

[4] Y. Masuda, D. Nagahama, H. Itahara, T. Tani, W. S. Seo, and K. Koumoto, "Thermoelectric performance of Bi- and Na-substituted $Ca_3Co_4O_9$ improved through ceramic texturing," *J. Mater. Chem.*, vol. 13, no. 5, pp. 1094–1099, Apr. 2003.

[5] L. Wu, Q. Meng, C. Jooss, J.-C. Zheng, H. Inada, D. Su, Q. Li, and Y. Zhu, "Origin of Phonon Glass–Electron Crystal Behavior in Thermoelectric Layered Cobaltate," *Adv. Funct. Mater.*, vol. 23, no. 46, pp. 5728–5736, Dec. 2013.

[6] G. Rijnders and D. H. A. Blank, "Materials science: Build your own superlattice," *Nature*, vol. 433, no. 7024, pp. 369–370, Jan. 2005.

[7] A. Sakai, T. Kanno, S. Yotsuhashi, S. Okada, and H. Adachi, "Preparation of metastable $Sr_3Co_4O_9$ epitaxial thin films with controlled orientation and their anisotropic thermoelectric properties," *J. Appl. Phys.*, vol. 99, no. 9, p. 093704, May 2006.

[8] V. Moshnyaga, I. Khoroshun, A. Sidorenko, P. Petrenko, A. Weidinger, M. Zeitler, B. Rauschenbach, R. Tidecks, and K. Samwer, "Preparation of rare-earth manganite-oxide thin films by metalorganic aerosol deposition technique," *Appl. Phys. Lett.*, vol. 74, no. 19, pp. 2842–2844, May 1999.

[9] M. Kawasaki, K. Takahashi, T. Maeda, R. Tsuchiya, M. Shinohara, O. Ishiyama, T. Yonezawa, M. Yoshimoto, and H. Koinuma, "Atomic Control of the $SrTiO_3$ Crystal Surface," *Science*, vol. 266, no. 5190, pp. 1540–1542, Dec. 1994.

[10] A. C. Masset, C. Michel, A. Maignan, M. Hervieu, O. Toulemonde, F. Studer, B. Raveau, and J. Hejtmanek, "Misfit-layered cobaltite with an anisotropic giant magnetoresistance: $Ca_3Co_4O_9$," *Phys. Rev. B*, vol. 62, no. 1, pp. 166–175, Jul. 2000.